

Integrated Microwave (Centimeter-Range) Modulator on Polycrystalline Diamond Layers

V. V. Basanets^a, N. S. Boltovets^a, A. V. Gutsul^a, A. V. Zorenko^a, V. G. Ral'chenko^b, A. E. Belyaev^c,
V. P. Klad'ko^c, R. V. Konakova^c*, Ya. Ya. Kudrik^c, A. V. Kuchuk^c, and V. V. Milenin^c

^a Orion State Research Institute, ul. Ezhena Pot'e 8a, Kyiv, 03680 Ukraine

^b Prokhorov General Physics Institute, Russian Academy of Sciences, ul. Vavilova 38, Moscow, 119991 Russia

^c Lashkarev Institute of Semiconductor Physics, National Academy of Sciences of Ukraine, pr. Nauki 45, Kyiv, 03028 Ukraine

*e-mail: konakova@isp.kiev.ua

Received November 24, 2011; in final form, April 16, 2012

Abstract—Measuring data for the parameters of a microstrip switching superhigh-frequency integrated circuit on a 100- μm -thick polycrystalline diamond film are reported. Measurements are taken in the frequency range 3–7 GHz. It is shown that the decay in developmental modulators is no greater than 1.5 dB in the on state and no less than 29 dB in the off state. Physicochemical analysis of the multilayer contact metallization technology as applied to synthetic diamond and a silicon p – i – n diode is carried out. The metallization is shown to be stable up to 400°C.

DOI: 10.1134/S1063784213030055

INTRODUCTION

The thermal conductivity and dielectric losses in the substrates of hybrid integrated circuits (ICs) play a decisive role in providing high performance and reliable operation of microwave devices [1, 2]. For centimeter- and millimeter-wave hybrid ICs, substrates made of artificial chemical vapor deposition (CVD) tungsten seem to be very promising. In these substrates, the thermal conductivity may be as high as 1800–2000 W/m K or even 3300 W/m K [3, 4] in isotope-free diamond and the dielectric loss tangent is very low (on the order of 10^{-5} at frequencies to 200 GHz) [5, 6].

The available methods of diamond film growth on silicon substrates are well adapted to semiconductor device fabrication. Topological feature mounting techniques can fully display the advantages of artificial diamond: very low dielectric losses in the substrate, low operating temperature of the p – i – n diode at high power modulation, and the stability of both parameters during long-term operation [7].

However, experimental data characterizing the functional parameters of microwave IC features on thick (about 100 μm) layers of synthetic diamond are today lacking. In this work, we carry out physicochemical analysis of patterning synthetic diamond layers and also present experimental parameters of the modulator in the frequency range 3–7 GHz.

1. SAMPLES AND INVESTIGATIVE TECHNIQUES

We studied a microwave IC fabricated by the method described in [7] and test structures intended

for physicochemical analysis of multilayer metallization in microwave elements (p – i – n diodes and transmission lines on synthetic diamond layers). Diamond layers 100–140 μm thick were CVD-grown on silicon substrates (Prokhorov General Physics Institute, Russian Academy of Sciences) using a microwave plasma to decompose CH_4 and H_2 reagents [8].

A microwave IC on a polycrystalline substrate (diamond film about 100 μm thick) was incorporated into a measuring module. After the IC was mounted on the diamond film, contact pads were connected to the input/output sockets of the microwave signal by soldering. Discrete inductances and capacitances aimed at discriminating microwave and low-frequency signals and current-limiting resistors were mounted between contact pads serving to apply power and control signals and a board for low-frequency fanout. Switching beam-leaded p – i – n diodes were mounted by thermocompression bonding.

The beam-leaded p – i – n diodes were fabricated by the method described in [9]. The surface p -Si layers were additionally doped by boron to a concentration on the order of 10^{20} cm^{-3} to form p^+ layers, and n^+ -Si layers were prepared by phosphorus doping to $1.8 \times 10^{20} \text{ cm}^{-3}$. Ohmic contacts were made exactly to these layers. After the p – i – n diodes were incorporated into the microwave IC, they provided a constant reverse voltage of no lower than 120 V at a current of 0.1 μA and a forward resistance of no more than 1.1 Ω at a current of 10 mA.

The transmission and attenuation coefficients of the microwave modulator were measured at several values of the forward current (on state) and reverse

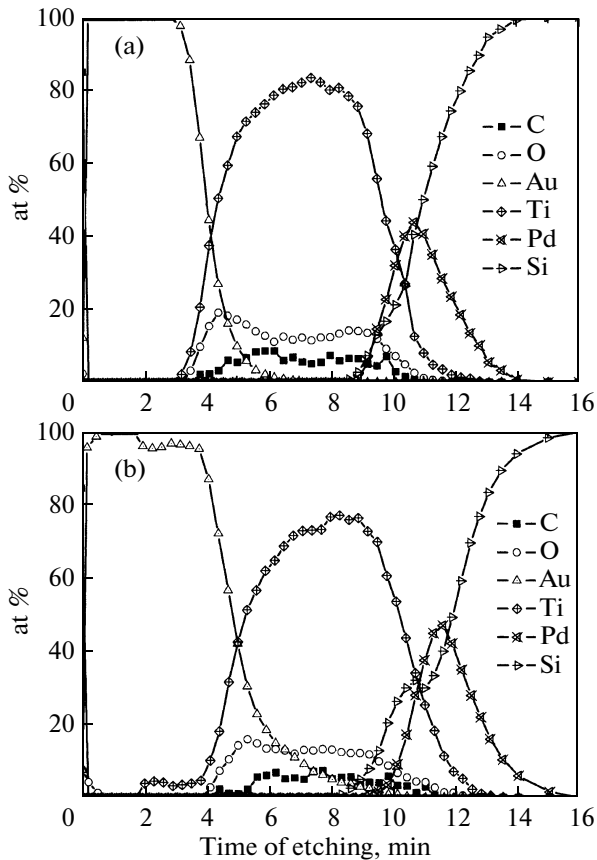


Fig. 1. Component distribution profile in the Au-Ti-Pd- n^+ -Si contact metallization in the (a) as-prepared sample and (b) sample heat-treated at 450°C for 10 min.

current (off state) through the $p-i-n$ diodes [10]. Measurements were taken with an R2-107 standing wave ratio and attenuation meter.

An LAS-2000 Auger spectrometer combined with ion etching (1-keV Ar^+ ions) was used to take the distribution of Pd(30 nm)-Ti(50 nm)-Au(120 nm) metallization components on $1 \times 1\text{-cm}^2$ test $p-i-n$ structures. The metallization, being the same for the p^+ - and n^+ -layers of the $p-i-n$ diode, was applied on the substrate heated to 330°C by vacuum evaporation. Metallization on the diamond was applied by successive vacuum evaporation of Ti (50 nm), Pd (100 nm), and Au (150 nm) layers on the substrate heated to 400°C. The phase composition of the metallization both on the $p-i-n$ structures and on the synthetic diamond was examined in situ by high-resolution X-ray diffraction using a Philips X'pert multipurpose diffractometer ($\text{CuK}\alpha$, $\lambda = 0.15418\text{ nm}$) in the Bragg-Brentano geometry. To check the thermal stability of the metallizations on the $p-i-n$ structures and synthetic diamond, they were heat-treated at 450°C for 10 min in vacuum.

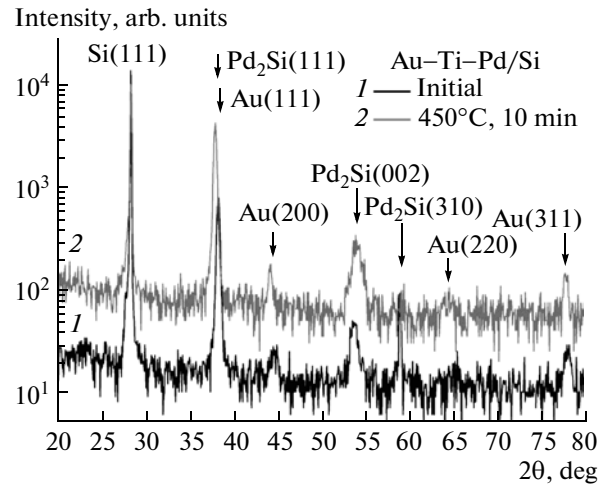


Fig. 2. X-ray diffraction patterns taken of the Au-Ti-Pd- n^+ -Si contact metallization for the (1) as-prepared sample and (2) sample heat-treated at 450°C for 10 min.

2. PHYSICOCHEMICAL ANALYSIS OF IC FEATURE FABRICATION ON SYNTHETIC DIAMOND LAYERS

2.1. Metallization of the $p-i-n$ Structure

It is known that palladium as-evaporated on a heated Si substrate or annealed on it forms an identical ohmic contact to the n - and p -regions [11, 12]. In this work, ohmic contacts with a contact resistivity of $\sim 10^{-6}\ \Omega\ \text{cm}^2$ were obtained by Pd evaporation and its parameters on the p^+ - and n^+ -layers of Si were really identical. The physicochemical properties of the contact metallization were also nearly the same. Therefore, the analytical results for these properties given below refer only to the contact to the n^+ -Si. From the component distributions in the initial sample (Fig. 1a) it follows that palladium silicide forms as early as in the course of palladium evaporation and the titanium film contains oxygen owing to the gettering properties of titanium. Together with oxygen, the titanium film contains carbon in an amount of 10%. The gold film is slightly diffused at the interface with the titanium, and the diffused region is enriched with oxygen and carbon. Heating at 450°C for 10 min (Fig. 1b) imitating the thermal overload of the $p-i-n$ diode intensifies or completes silicide formation at the interface with the silicon and causes mass transfer in all metallization layers. In this case, the silicon distribution profile exhibits a step, the titanium penetrates into the gold film to half its thickness, and gold mass transfer up to the interface with the silicon is observed.

The phase composition of the Au-Ti-Pd- n^+ -Si contact metallization both as-prepared and heat-treated at 450°C for 10 min is presented in Fig. 2. It is seen that the only phase resulting from the palladium evaporation on the heated silicon substrate and persisting after heat treatment is Pd_2Si , which provides an

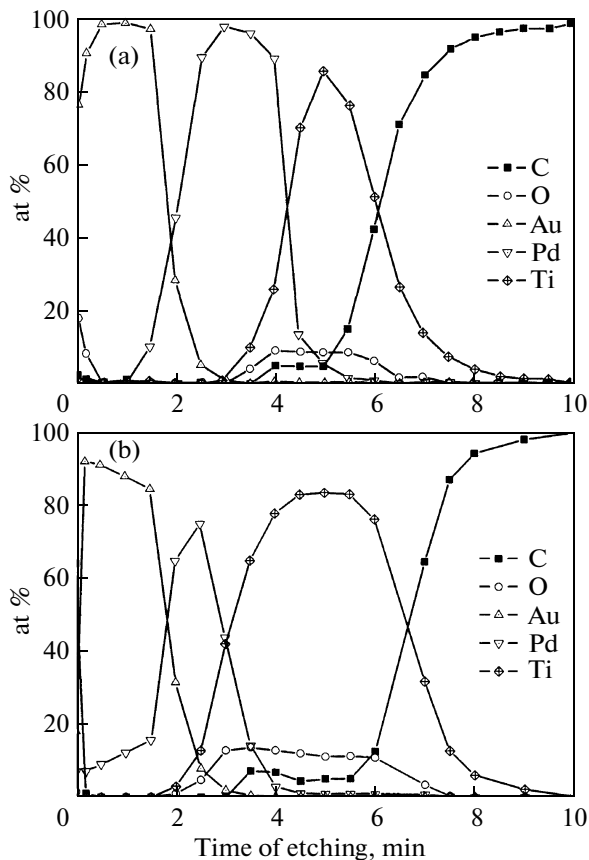


Fig. 3. Component distribution profile in the Au–Pd–Ti–C metallization in the (a) as-prepared sample and (b) sample heat-treated at 450°C for 10 min.

ohmic contact to the silicon [13]. Along with the (111), (002), and (310) reflections from Pd_2Si , the (111) reflection from Si and the (111), (200), (220), and (311) reflections from the Au film are observed in the as-prepared and heat-treated samples. However, the reflections from the Ti film are absent. This may be associated with the so-called roentgen-amorphous state of the titanium having metallic conduction, as indicated by the non-increased contact resistivity upon heat treatment.

2.2. Metallization of Synthetic Diamond

The distribution of the components of metallization to the synthetic diamond is shown in Figs. 3a and 3b. It is seen that the initial (as-prepared) sample (Fig. 3a) has layered metallization. In the Ti film, as well as in the contact to the $n^+(p^+)\text{-Si}$, oxygen and carbon are present. Heat treatment at 400°C for 10 min changes the layered structure of the contact metallization insignificantly. At the same time, heat treatment at 450°C for 10 min (Fig. 3b) causes intense mass transfer of titanium into the Pd film and the emergence of palladium on the surface of the gold film. However, the Ti–diamond interface does not experi-

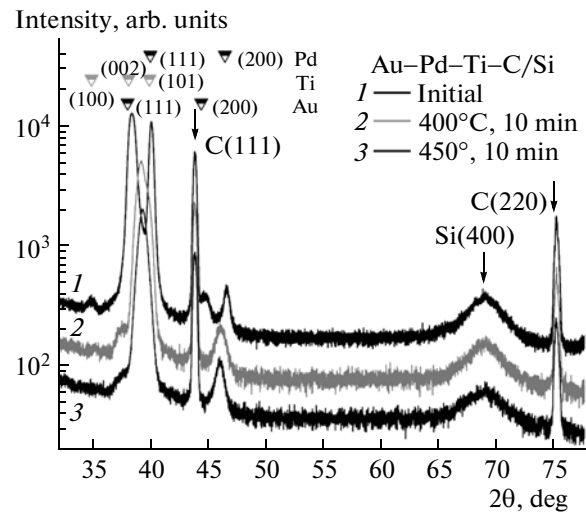


Fig. 4. X-ray diffraction patterns taken of the Au–Pd–Ti–C–Si structure for the (1) as-prepared sample, (2) sample heat-treated at 400°C for 10 min, and (3) sample heat-treated at 450°C for 10 min.

ence considerable changes. The variation of Au, Ti, and Pd distribution profiles indicates the possibility of forming a solid solution consisting of these components.

High-resolution X-ray diffraction data for the metallization to the diamond are shown in Fig. 4. The high-resolution X-ray diffraction spectra taken of the initial Au–Pd–Ti–C–Si contact (curve 1) contain the (400) reflection from Si; (111) and (220) reflections from C; (111) and (200) reflections from Au; (111) and (200) reflections from Pd; and (100), (002), and (101) reflections from Ti. This series of reflections from the metallization suggests the polycrystalline structure of Au, Pd, and Ti layers. The high-resolution X-ray diffraction spectra taken of the Au–Ti–Pd–C–Si contact annealed at 400°C (curve 2) contain, along with reflections from silicon and diamond, two more reflections at 39 and 46°C). Their corresponding lattice parameter, which is larger than for bcc Pd but smaller than for bcc Au, indicates the formation of a solid solution consisting of Au, Ti, and Pd. The asymmetry of these two reflections (overlaps on both sides) indicates that the fractions of pure Au, Ti, and Pd metals are small and also that the process of phase formation is not completed. The asymmetry of these reflections disappears after heat treatment at 450°C (curve 3) presumably because of more intense interdiffusion of atoms along grain boundaries with the formation of $\text{Au}_x(\text{Ti}, \text{Pd})_{1-x}$ solid solution.

It also follows from Fig. 4 that heat treatment does not change the structure of the polycrystalline diamond film. The constancy of the diffraction peak positions and their full width at half maximum (FWHM) indicate that the stability of the lattice (the absence of considerable internal mechanical stresses)

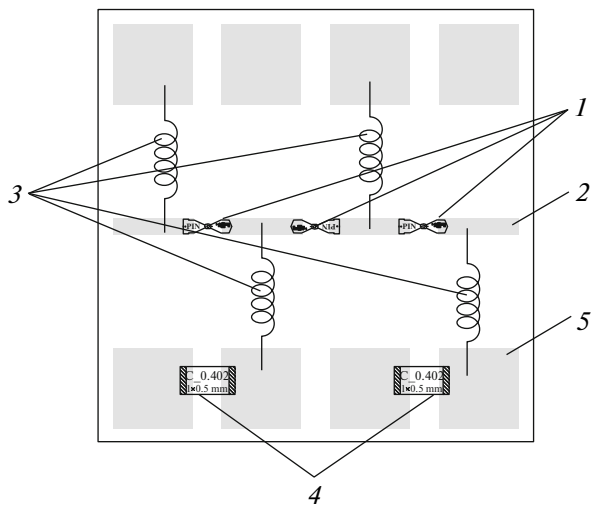


Fig. 5. Layout of the microstrip microwave switching IC on the synthetic diamond substrate: (1) switching silicon *p-i-n* diodes, (2) microstrip transmission line ($Z_w = 50 \Omega$), (3) inductances, and (4) capacitors, and (5) synthetic diamond substrate.

and coherent scattering regions ~ 25 nm across in diamond crystallites.

The above physicochemical analysis of the contact metallization suggests that a more effective diffusion barrier should be provided between the Au film and contact-forming metal to suppress mass transfer of Pd in the Au–Pd–Ti–C contact and Ti in the Au–Ti–Pd– n^+ –Si contact and retain the layered structure of the contact metallization at temperatures above 400°C. Diffusion barriers based on heat-resistant refractory metal boride and nitride interstitials seem to be the most promising [11, 14].

It should also be noted that the metallization systems for the *p-i-n* diode and synthetic diamond were heat-treated at 400°C for 5 min to model the conditions of microsoldering and flux-free bonding.

3. RESULTS AND DISCUSSION

The microstrip microwave switching hybrid IC (Fig. 5) is designed so as to provide the possibility of applying a control voltage to the *p-i-n* diodes and connecting them back to back. With such a connection, sections of the microstrip line can be alternately connected to a grounded conductor and to a power supply. This is accomplished using inductances, which do not influence the passage of the microwave signal through the switching IC and, at the same time, provide the passage of low-frequency bias currents through the *p-i-n* diodes.

At the edges of the IC, contact pads are made to apply control voltages and to mount filter capacitors. The contact pads are squares measuring 1.5×1.5 mm, which suffices to mount all necessary IC features.

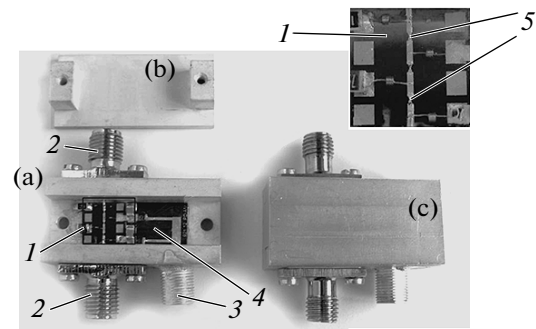


Fig. 6. Two microwave ICs on the diamond substrate inserted in measuring modules: (a) measuring module with the IC, (b) lid, and (c) assembled measuring module with the IC. (1) microwave chip on the diamond substrate, (2) input/output of the microwave signal, (3) input of the *p-i-n* diode control signal, (4) *p-i-n* diode supply board, and (5) silicon *p-i-n* diodes integrated into the microwave IC.

The measured parameters of the modulator (Fig. 6) are listed in the table. It follows from the table that, for a direct total current through three diodes of 30 mA in the on state, the losses of the module are within 1.5 dB in the frequency range 3–7 GHz and within 0.5 dB in the range 5–7 GHz. In the off state (a reverse voltage of 10 V), the attenuation is 29 dB or greater. One can see that the losses of the modulator in the on state and its attenuation in the off state compare favorably with those of similar devices known today, specifically, with those of a commercial HMC346G8 GaAs modulator (Hittite Microwave Corporation) [15]. The transmission losses, attenuation, operating frequency range, and operating temperature range of the HMC346G8 modulator are, respectively, 2 dB, 30 dB, 0.1–8.0 GHz, and 40–85°C. However, the modulator on the synthetic diamond substrate can operate much longer at high ambient temperatures than commercial modulators. This is due to the record high thermal conductivity of diamond and also follows from the results of imi-

The attenuation/transmission factor of the microwave modulator at different frequencies for forward-(reverse-)biased *p-i-n* diodes

Frequency f , GHz	Attenuation (transmission) factor L , dB		
	forward-biased <i>p-i-n</i> diodes, bias current	reverse-biased <i>p-i-n</i> diodes, bias voltage	
		$I = 30$ mA	$U = 0$ V
3.0	–1.5	–28	–32
4.0	–1.0	–29	–33
5.0	–0.5	–28	–32
6.0	–0.4	–26	–30
7.0	–0.3	–25	–30

tating heat treatments of the metallized polycrystalline diamond (see Section 2), which confirm the thermal stability of metallization and diamond film.

Thus, it was shown that $p-i-n$ diode-based centimeter-wave modulators with parameters suitable for applications can be fabricated on thin films of synthetic diamond. Such modulators are of great interest for switching elevated microwave powers owing to the high thermal conductivity of the diamond film and the feasibility of their commercial production.

CONCLUSIONS

(i) A Ti–Pd–Au metallization system for a diamond substrate and a Pd–Ti–Au system for a silicon $p-i-n$ diode demonstrate high thermal stability necessary to withstand microsoldering and flux-free bonding at temperatures up to 400°C.

(ii) The attenuation in developmental modulators in the frequency range 3–7 GHz does not exceed 1.5 dB in the on state and is no less than 30 dB in the off state, which makes promising fabrication of such devices on thin layers of synthetic diamond.

REFERENCES

1. V. I. Molchanov and Yu. M. Poplavko, *Fundamentals of Microwave Electronics* (NTUU KPI, Kiev, 2010).
2. Y. Liao Samuel, *Microwave Devices and Circuits* (Prentice Hall, Singapore, 1997).
3. A. V. Sukhadolau, E. V. Ivakin, V. G. Ralchenko, A. V. Khomich, A. V. Vlasov, and A. F. Popovich, *Diamond Relat. Mater.* **14**, 589 (2005).
4. J. R. Olson, R. O. Pohl, J. W. Vandersande, A. Zoltan, T. R. Anthony, and W. F. Banholzer, *Phys. Rev. B* **47**, 14850 (1993).
5. B. M. Garin, A. N. Kopnin, V. V. Parshin, V. G. Ralchenko, E. E. Chigryai, V. I. Konov, A. B. Mazur, and M. P. Parkhomenko, *Tech. Phys. Lett.* **25**, 288 (1999).
6. *Element six. Inc.* www.cvd-diamond.com.
7. N. S. Boltovets, A. E. Belyaev, R. V. Konakova, T. V. Korostinskaya, V. A. Krivutsa, O. S. Litvin, V. V. Milenin, A. P. Bol'shakov, and V. G. Ral'chenko, *Tekhn. Prib. SVCh*, No. 2, 26 (2009).
8. V. G. Ral'chenko, A. V. Savel'ev, A. F. Popovich, I. I. Vlasov, S. V. Voronina, and E. E. Ashkinazi, *Mikroelektronika* **35**, 243 (2006).
9. N. S. Boltovets, V. V. Basanets, T. I. Golynnaya, V. A. Krivutsa, L. M. Suvorova, and K. A. Lychman, *Tekhn. Prib. SVCh*, No. 2, 34 (2008).
10. Ishi Thomas Koryu, *Handbook of Microwave Technology: Components and Devices* (Academic, New York, 1995).
11. D. G. Gromov, A. I. Mochalov, A. D. Sulimin, and V. I. Shevyakov, *Metallization of Ultralarge-Scale Integration* (Binom, Moscow, 2011).
12. S. P. Murarka, *Silicides for VLSI Applications* (Academic, San Diego, 1983).
13. A. E. Belyaev, V. V. Basanets, N. S. Boltovets, A. V. Zorenko, L. M. Kapitanchuk, V. P. Klad'ko, R. V. Konakova, N. V. Kolesnik, T. V. Korostinskaya, T. V. Kritskaya, Ya. Ya. Kudrik, A. V. Kuchuk, V. V. Milenin, and A. B. Ataubaeva, *Semiconductors* **45**, 253 (2011).
14. O. A. Ageev, A. E. Belyaev, N. S. Boltovets, R. V. Konakova, V. V. Milenin, and V. A. Pilipenko, *Interstitial Phases in Technology for Semiconductor Devices and VLSI*, Ed. by R. V. Konakova (NTK Inst. Monokrist., Khar'kov, 2008).

Translated by V. Isaakyan